

# Age- and function-related regional changes in cortical folding of the default mode network in older adults

Christiane Jockwitz<sup>1,2</sup> · Svenja Caspers<sup>1,2</sup> · Silke Lux<sup>2</sup> · Kerstin Jütten<sup>2</sup> · Axel Schleicher<sup>2</sup> · Simon B. Eickhoff<sup>2,3</sup> · Katrin Amunts<sup>1,2</sup> · Karl Zilles<sup>2,4,5</sup>

Received: 11 August 2015 / Accepted: 9 February 2016 / Published online: 4 March 2016  
© Springer-Verlag Berlin Heidelberg 2016

**Abstract** Healthy aging is accompanied by changes in the functional architecture of the default mode network (DMN), e.g. a posterior to anterior shift (PASA) of activations. The putative structural correlate for this functional reorganization, however, is largely unknown. Changes in gyrification, i.e. decreases of cortical folding were found to be a marker of atrophy of the brain in later decades of life. Therefore, the present study assessed local gyrification indices of the DMN in relation to age and cognitive performance in 749 older adults aged 55–85 years. Age-related decreases in local gyrification indices were found in the anterior part of the DMN [particularly; medial prefrontal cortex (mPFC)] of the right hemisphere, and the medial posterior parts of the DMN [particularly; posterior cingulate cortex (PCC)/precuneus] of both hemispheres. Positive correlations between cognitive performance and local gyrification indices were found for (1) selective attention and left PCC/precuneus, (2) visual/visual–spatial working memory and bilateral PCC/precuneus and right angular gyrus (AG), and (3) semantic verbal fluency and

right AG and right mPFC. The more pronounced age-related decrease in local gyrification indices of the posterior parts of the DMN supports the functionally motivated PASA theory by correlated structural changes. Surprisingly, the prominent age-related decrease in local gyrification indices in right hemispheric ROIs provides evidence for a structural underpinning of the right hemi-aging hypothesis. Noticeably, the performance-related changes in local gyrification largely involved the same parts of the DMN that were subject to age-related local gyrification decreases. Thus, the present study lends support for a combined structural and functional theory of aging, in that the functional changes in the DMN during aging are accompanied by comparably localized structural alterations.

**Keywords** Aging · Gyrification · Default mode network · Cognition

## Introduction

Aging is associated with changes in functional brain networks, such as the default mode network (DMN) (Andrews-Hanna et al. 2007; Bai et al. 2008; Damoiseaux et al. 2008; Mevel et al. 2011). The DMN is a bilaterally distributed functional brain network (Schilbach et al. 2012) consisting of an anterior [medial prefrontal (mPFC) and anterior cingulate cortex (ACC)], as well as a medial [posterior cingulate cortex (PCC) and precuneus] and lateral posterior part (inferior parietal lobule and parts of the temporal lobe). It is characterized by its activation during phases of rest, while it is deactivated (or suppressed) during externally focused states, and is associated with a variety of cognitive functions, such as attention, self-referential

✉ Svenja Caspers  
svenja.caspers@hhu.de

<sup>1</sup> C. & O. Vogt Institute for Brain Research, Heinrich Heine University, 40225 Düsseldorf, Germany

<sup>2</sup> Institute of Neuroscience and Medicine-1, Research Center Jülich, 52425 Jülich, Germany

<sup>3</sup> Institute Clinical Neuroscience and Medical Psychology, University of Düsseldorf, Düsseldorf, Germany

<sup>4</sup> JARA-Brain, Jülich-Aachen Research Alliance, Jülich, Germany

<sup>5</sup> Department of Psychiatry, Psychotherapy and Psychosomatics, RWTH Aachen University, Aachen, Germany

cognition, episodic and working memory (Buckner et al. 2008; Raichle et al. 2001; Amft et al. 2015).

In the course of aging, several studies revealed changes in functional connectivity within the DMN (Andrews-Hanna et al. 2007; Batouli et al. 2009; Damoiseaux et al. 2008; Mowinckel et al. 2012; Wu et al. 2011). For example, Andrews-Hanna et al. (2007) reported a decrease of the functional coupling during task performance between the mPFC and PCC/precuneus in older compared to younger adults, making the two parts more independent from each other. Accordingly, age-related increases in resting-state functional connectivity were reported for the anterior DMN but not the posterior DMN in older subjects (Jones et al. 2011). Similar effects were found during task-based functional imaging. Older subjects were found to show less deactivation within the PCC/precuneus as compared to the mPFC (Davis et al. 2008; Grady et al. 2006; Lustig et al. 2003). Thus, a shift in (de-) activation from posterior to anterior brain regions in aging (PASA) might be present in older adults that serves as a compensatory mechanism to maintain cognitive performance as stable as possible (Davis et al. 2008; Grady et al. 1994).

While there is evidence for a functional reorganization of the DMN in terms of PASA, differences in hemispheric asymmetries regarding age-related decline have not been explored yet. Investigating young adults, first studies showed that there might be hemispheric differences in functional connectivity of the DMN (Saenger et al. 2012). Regarding cognitive decline in the course of aging, it is established that not all cognitive functions decrease at the same rate from early to late adulthood (Hedden and Gabrieli 2004). Dolcos (2002) for example discussed whether there are differences in the aging processes of the left as compared to the right hemisphere. The right hemi-aging theory states that the right hemisphere is more prone to age-related decline (Grady et al. 1994). This, in turn, would result in an earlier decrease of cognitive functions that are predominantly processed within the right hemisphere, such as visual–spatial functions. In terms of age-related structural changes of the DMN, a more pronounced structural decrease of right hemispheric parts would be reasonable. Thus, based on functional imaging and behavioral research evidence exists that age-related reorganization of the DMN might happen along a posterior–anterior (PASA) as well as right–left axis (right hemi-aging).

While there is evidence for a functional reorganization of the DMN, the question of the possible underlying structural correlate is still unresolved. To assess the structural correlates of the DMN, gyrification, i.e. degree of cortical folding is a valuable measure for studying changes of brain structure. Driven mainly by cell proliferation and migration as well as fiber connectivity, it is supposed to

reflect the underlying structural connectivity and complexity (for a recent review: Zilles et al. 2013, 2015), particularly as a measure of local atrophy in later decades of life (Kochunov et al. 2005; Magnotta et al. 1999; Van Essen 1997; Welker 1990; Zilles et al. 1988). The gyrification index (GI) as a measure of the degree of cortical folding was introduced by Zilles et al. (1988) as a contour-based two-dimensional (2D) approach to measure gyrification in post-mortem brains. The ratio between the total outer cortical contour length and that of the superficially exposed part of the cortex, which does not comprise the segments buried in the sulci, defines the GI: the higher the GI, the higher the degree of cortical folding. A three-dimensional (3D) extension of the original GI was developed by Schaer et al. (2008) using the reconstructed surface from in vivo T1-weighted brain images. The so-called local gyrification index is calculated over thousands of vertices. Several studies used the method of Schaer et al. (2008) to study changes in local gyrification indices with respect to development and aging, cognitive abilities as well as diseases such as schizophrenia, psychosis and Parkinson's disease (Palaniyappan and Liddle 2012; Docherty et al. 2015; Palaniyappan et al. 2013; White et al. 2010; Zhang et al. 2014). With respect to healthy aging, Hogstrom et al. (2013) were able to show age-related regional decreases in local gyrification within, e.g. the postcentral gyrus and inferior parietal lobules.

Taken together, based on functional imaging the DMN has been shown to be susceptible to age-related functional reorganization, such as the PASA from early to late adulthood. By contrast, potential structural correlates of this age-related functional reorganization of the DMN have not been identified yet. In the present study, we implemented measures of the local gyrification index as a marker of age-related structural atrophy within the DMN. We investigated the relation between local gyrification indices within different parts of the DMN and age as well as cognitive performance in 749 older adults. It was hypothesized that, in line with the PASA theory, age-related structural decline would be more pronounced in posterior parts of the DMN as compared to the anterior parts of the DMN. In addition, according to the right hemi-aging theory, we hypothesized that the right hemispheric parts of the DMN would be more prone to age-related structural decline as compared to the left hemispheric parts of the DMN.

## Methods

### Subjects

Data of all subjects included in the present study (age range: 55–85 years) were derived from 1000BRAINS

(Caspers et al. 2014), an epidemiologic population-based study assessing the variability of brain structure and function in the course of normal aging, based on the epidemiologic population-based Heinz Nixdorf Recall Study with focus on risk factors for atherosclerosis, cardiovascular disease, cardiac infarction and death (Schmermund et al. 2002). From the initial sample of 989 subjects, 843 subjects were aged between 55 and 85 years. Complete T1-weighted MRI data sets were available for 792. Two subjects had to be excluded from the analysis due to considerable structural brain defects post stroke. 25 subjects had to be excluded due to postprocessing failure within FreeSurfer (see below) and another 16 subjects had more than three tests that were not executed during the neuropsychological assessment and therefore were excluded as well. Finally, 749 subjects (mean age: 67.24, SD: 6.78, 413 males, 336 females) were eligible for the structural analysis of the gyrification index. All subjects gave written informed consent at the beginning of the study. The study protocol was approved by the local Ethics Committee of the University of Essen.

### Image acquisition

Brain imaging data were acquired on a 3T Siemens Tim-TRIO MR scanner (Erlangen, Germany), using a 32-channel head coil. For the surface reconstruction, a 3D high-resolution T1-weighted magnetization-prepared rapid acquisition gradient-echo (MPRAGE) anatomical scan was acquired in each subject (176 slices, slice thickness 1 mm, repetition time (TR) = 2250 ms, echo time (TE) 3.03 ms, field of view (FoV) =  $256 \times 256 \text{ mm}^2$ , flip angle =  $9^\circ$ , voxel resolution  $1 \times 1 \times 1 \text{ mm}^3$ ). For the resting-state analyses, as used here for the extraction of the DMN, 300 functional images were acquired at rest using a gradient-echo echo planar imaging (EPI) sequence (36 slices, slice thickness 3.1 mm, TR = 2200 ms, TE = 30 ms, FoV =  $200 \times 200 \text{ mm}^2$ , voxel resolution  $3.1 \times 3.1 \times 3.1 \text{ mm}^3$ ). During the resting state condition, subjects were instructed to keep their eyes closed, relax, let their minds wander, but not to fall asleep. This was affirmed by post-scan debriefing.

### Definition of the DMN seed regions on resting-state fMRI data

Image analysis was performed using FSL [FMRIB Software Library: <http://www.fmrib.ox.ac.uk/fsl>; (Jenkinson et al. 2012)]. For every subject, preprocessing included motion correction [MCFLIRT; (Jenkinson et al. 2002)], brain extraction [BET; (Smith 2002)], and high pass temporal filtering (100 ms). FMRIB's Linear and Nonlinear Image Registration tool [FLIRT and FNIRT; (Jenkinson et al. 2002; Jenkinson and Smith 2001)] were used to

register the participant's resting state-fMRI volumes to the individual structural scan. The latter was registered to the standard space template (MNI 152). Then, all images were smoothed by a 5-mm FWHM Gaussian kernel. For every subject, EPI images were denoised using FMRIB's ICA-based Xnoiseifier and corrected for motion artefacts [FIX; (Griffanti et al. 2014; Salimi-Khorshidi et al. 2014)]. Finally, EPI images were resampled at 3 mm isotropic voxel size.

After preprocessing, MELODIC multi-session temporal concatenation (Beckmann et al. 2005) was used to identify common spatial patterns across subjects within the resting state data using probabilistic independent component analysis decomposition of the resting state signals (Beckmann and Smith 2004). Subjects for this study were selected based on availability of structural MRI data to increase sample size. Since not all subjects also completed the resting state scan, a bootstrapping approach was used to reliably define the DMN across the whole sample [similar to other approaches, such as ICASSO, which uses a clustering to reliably extract resting state networks (Himberg and Hyvarinen 2003)]: Resting state datasets were available for 691 subjects. From this subsample 200 subjects were randomly selected using a random number generator. Resting state networks were extracted from the group of 200 randomly selected subjects using MELODIC. DMN was selected via visual inspection to identify the best spatial match to the DMN as published by Beckmann and Smith (2004) and Smith et al. (2009). This procedure was repeated 100 times (Fig. 1a), giving 100 DMNs, each based on a random sample of 200 subjects. Afterwards, the extracted 100 DMNs were superimposed onto each other in standard MNI space. This resulted in a DMN probability map, expressing the likelihood of a brain region to be involved in the DMN (ranging from 0 to 100 %) (Fig. 1b). The probability map was then thresholded at 95 % (using *fslmaths*, FSL), meaning that only if 95 out of the 100 DMNs included a given brain area, it was included into the final definition of the DMN (Fig. 1c). Each ROI was finally represented by its center of gravity (Fig. 1d). These final ROIs as defined in MNI-152 space were transformed into each subject's individual space (using FNIRT/FLIRT as implemented in FSL) to allow for subsequent surface-based extraction of the local GI by means of FreeSurfer (Fig. 1i).

### ROIs of the DMN

The resulting mean DMN, averaged over all permutations and thresholded at 95 %, consisted of six clusters: Two anterior and four posterior clusters: (1) left mPFC (2) right mPFC (3) left PCC/precuneus, (4) right PCC/precuneus,

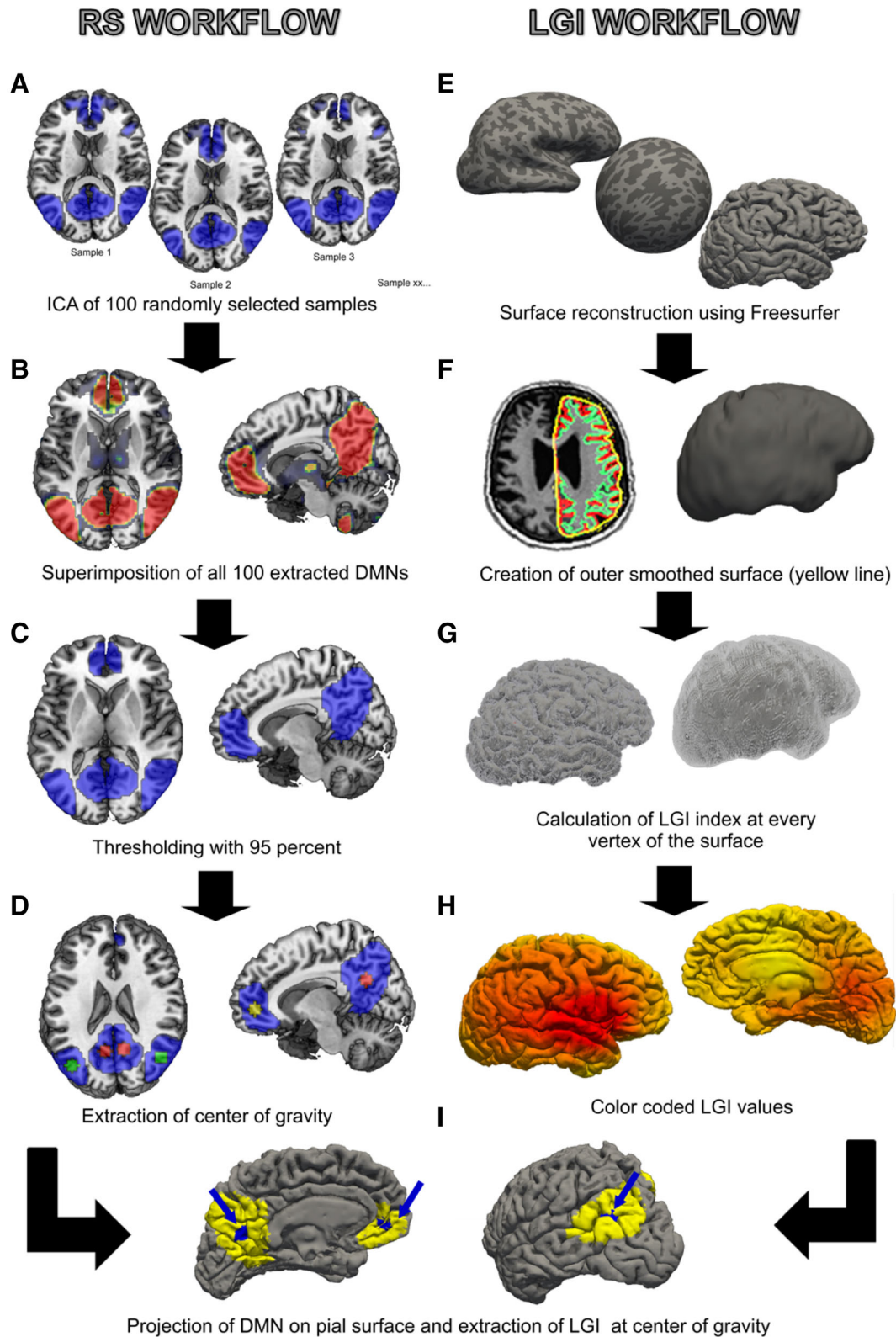


**Fig. 1** *Left panel* resting state (RS) workflow. Extraction of DMN, superimposition of all extracted DMNs, thresholding and projection on pial surface. *Right panel* local gyrification index (LGI) workflow.

Freesurfer pipeline and calculation of local gyrification index (LGI; of every vertex on the pial surface and ROI)

(5) left AG (left angular gyrus), and (6) right AG. Figure 2 provides an overview of these six DMN-ROIs including macroanatomical and cytoarchitectonical identification of brain areas according the JuBrain Cytoarchitectonic Atlas (<http://jubrain.fz-juelich.de>) (Zilles and Amunts 2010), as implemented in the SPM Anatomy Toolbox (Eickhoff et al. 2005). Cytoarchitectonic areas were denoted in accordance with the respective publications (Amunts et al. 2000; Bludau et al. 2014; Caspers et al. 2008; Caspers et al. 2006; Kujovic et al. 2013; Malikovic et al. 2007; Palomero-Gallagher et al. 2015; Scheperjans et al. 2008a, b).

### Surface reconstruction and local gyrification index

Anatomical images were first preprocessed using SPM8 (Statistical Parametric Modeling: [www.fil.ion.ucl.ac.uk/spm](http://www.fil.ion.ucl.ac.uk/spm)). All anatomical images were segmented into grey matter, white matter, and cerebrospinal fluid. Grey and white matter images were combined to generate a reliable brain mask for subsequent processing within the FreeSurfer pipeline. Afterwards, all skull stripped images were processed using the cortical reconstruction pipeline implemented in FreeSurfer 5.1.0 [<http://freesurfer.net/>, (Dale et al. 1999; Fischl et al. 1999)]. This included transformation to Talairach space, and segmentation of grey and white matter tissue, tessellation of grey/white matter boundary and correction of topological defects. The grey/white matter interface was expanded to create the pial surface, followed by spherical morphing and registration (Fig. 1e). Local gyrification indices in native space were calculated according to Schaer et al. (2008, 2012) as

implemented in FreeSurfer. While the pial surface was already generated in the standard processing pipeline of FreeSurfer, the outer hull had to be created for calculation of the local gyrification index (also implemented in FreeSurfer; Schaer et al. 2008, 2012). This was achieved by tightly warping the pial surface by means of a morphological closing operation that uses a 15 mm sphere to close every sulcus (Fig. 1f). For each vertex of the pial surface, a local gyrification index value was assigned, calculated as the ratio of the pial surface area (defined as a sphere with the vertex as center and a 25 mm radius, according to Schaer et al. 2008) to the outer hull (Fig. 1g, h). Finally, local gyrification index was extracted for the vertices at the position of the center of gravity to best represent the gyrification over the whole extent of the ROI (Fig. 1i).

Surface reconstructions were randomly controlled for the participants. We did not find any systematic bias in the current data that would, in turn, bias the results on the local gyrification index measure. Further, all transformations of the DMN onto the individual subjects were controlled. Subjects for whom the transformations were not satisfactory were excluded from further analysis. In total, 25 subjects had to be excluded due to failure within FreeSurfer preprocessing and transformations from MNI to single subject space, which was mainly due to motion artefacts.

### Cognitive performance

All subjects underwent extensive neuropsychological assessment [for an overview: see Caspers et al. (2014)]. Detailed description of all cognitive functions measured,

**Fig. 2** Description of brain areas involved within the DMN, including macroanatomical and cytoarchitectonical identification of brain areas according the JuBrain Cytoarchitectonic Atlas

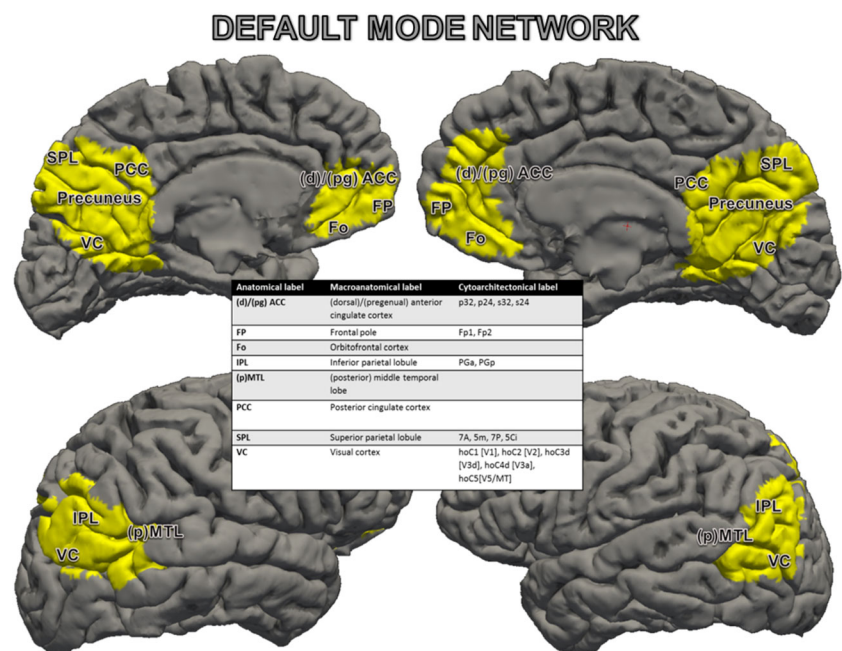


**Table 1** Overview of cognitive functions, tests and variables used, together with mean test scores and standard deviations (SD)

Cognitive function	Test	Variables	Mean (raw score)	SD
Selective attention	Alters-Konzentrations-test (Gatterer 2008)	Time (s) to find and cross out target items	34.77	11.49
Processing speed	Trail Making test (part A) (taken from CERAD-Plus; Morris et al. 1989)	Time (s) to connect randomly arranged digits in ascending order	40.46	17.11
Susceptibility to interference	Farb-Wort-Interferenztest (Jülich version; similar to: Stroop 1935; Bäumlner 1985)	Time difference (s) between naming the ink that color words were printed in (part 3) and reading color words (part 2)	43.65	24.11
Figural fluency	Fünf-Punkte-test (Jülich version; similar to: Regard et al. 1982)	Total number of unique patterns designed by connecting five dots within 3 min	26.30	7.89
Problem solving	Leistungsprüfungssystem 50 + (subtest 3) (Sturm et al. 1993)	Total number of correctly identified irregularities in rows of geometric figures within 5 min	20.55	5.17
Concept shifting	Trail making test (taken from CERAD-Plus; Morris et al. 1989)	Time difference (s) between connecting alternately numbers and letters in ascending order (part B) and randomly arranged digits in ascending order (part A)	56.26	44.08
Vocabulary	Wortschatztest (Schmidt and Metzler 1992)	Total number of correctly identified real words within rows of five pseudowords	30.79	4.98
Phonemic verbal fluency	Regensburger Wortflüssigkeitstest (Aschenbrenner et al. 2000)	Total number of produced words beginning with the letter “B” in 2 min	18.61	6.57
Semantic verbal fluency	Regensburger Wortflüssigkeitstest (Aschenbrenner et al. 2000)	Total number of produced words belonging to the category “Berufe (job)” in 2 min	23.85	6.80
Figural memory	Benton-test (Benton et al. 2009)	Total number of errors made during the free recall of 20 previously presented figures	16.86	8.41
Verbal learning	Verbaler Gedächtnistest (Lux et al. 2012)	Total number of free recalled words in 5 trials from a list containing 15 words	41.48	10.43
Visual spatial working memory	Block-tapping-test (Schelling 1997)	Total number of blocks given in a sequence which were correctly repeated (sum score forward and backward)	11.36	2.95
Visual working memory	Visual pattern (Jülich version; similar to: Della Sala et al. 1997)	Total number of memorized patterns given as a matrix of black and white squares with increasing complexity	7.70	1.78
Verbal working memory	Zahlennachsprechen (from Nürnberger Alters-Inventar; Oswald and Fleischmann 1997)	Total number of digits given in a sequence which were correctly repeated (sum scores forward and backward)	14.60	3.23

tests included and variables chosen are provided in Table 1. For subjects having not more than 3 missing values in the neuropsychological assessment (>3 missing values led to exclusion, see above), the missing values were replaced by the median (matched for gender and age decades: 55–64, 65–74, 75–85 years). Performance tests included in the present study covered measures of 14 distinct cognitive functions: selective attention, processing speed, susceptibility to interference, figural fluency, problem solving, concept shifting, vocabulary, verbal fluency (semantic and phonemic versions), figural memory and verbal learning as well as visual, visual–spatial and verbal working memory.

### Statistical analysis

The overall relation between age and local gyrification indices in parts of the DMN was analyzed using multivariate ANCOVA (Analysis of CoVariance) with gender as covariate. Afterwards, post hoc partial correlation analyses were carried out to assess the influence of age on every single part of the DMN after correcting for gender. Reported results were significant at  $p < .05$ , corrected for multiple comparisons using the false discovery rate [FDR; (Benjamini and Hochberg 1995)].

For the relation between cognitive performance and local gyrification indices in parts of the DMN, the

following steps were executed: First, all neuropsychological variables were rank-transformed as they were not normally distributed. Afterwards, the ranks were transformed into standard scores (using mean centering and scaling). We then calculated partial correlations between cognitive function scores and local gyrification indices while correcting for gender and age. All reported correlation results were significant at  $p < .05$ , FDR-corrected for multiple comparisons across the number of neuropsychological variables and brain regions. Finally, differences of correlation strength were tested for statistical significance using an adaptation of Steiger's  $Z$  (Steiger 1980; Hoerger 2013).

Subsequently, we re-ran all analysis by including the total score of the dementia screening test [DemTect, Kalbe et al. (2004)] as a covariate. Further, for the subsequent analysis of cognitive performance, we additionally excluded all subjects with missing values.

## Results

### Effects of age

To test for age-related changes of gyrification within the DMN, local gyrification indices for each part of the DMN were extracted. A three-way ANCOVA was applied to test for the effects of age and gender on local gyrification indices within the parts of the DMN and the interaction between ROI and age and gender. Afterwards a post hoc partial correlation analysis was conducted to investigate the effects of age on local gyrification indices for each part of the DMN while correcting for the effects of gender.

Three-way ANCOVA using ROI, age and gender as factors revealed significant main effects for ROI ( $F = 106.28$ ,  $p < .001$ ,  $df = 5$ ), and age ( $F = 34.26$ ,  $p < .001$ ,  $df = 1$ ), but not for gender ( $F = .98$ ,  $p = .3228$ ,  $df = 1$ ). Further, the interaction between age and ROI was significant ( $F = 3.68$ ,  $p = .0025$ ,  $df = 5$ ). No significant interaction between ROI and gender ( $F = .73$ ,  $p = .5988$ ,  $df = 5$ ), age and gender ( $F = .09$ ,  $p = .7607$ ,  $df = 1$ ) or ROI, age and gender was found ( $F = .39$ ,  $p = .8593$ ,  $df = 5$ ). Thus, the influence of age on ROI was further analyzed using partial correlation analyses (gender as covariate).

Post hoc partial correlation analysis (FDR-corrected for multiple comparisons) revealed heterogeneous relations between local gyrification indices and age for the different parts of the DMN. Local gyrification index of the right mPFC showed decreases with age ( $r = -.128$ ;  $p = .0004$ ; Fig. 3d), while there was no significant effect of age on local gyrification index in the left mPFC ( $r = .015$ ;  $p = .6853$ ; Fig. 3a). For the posterior parts of the DMN, we found significant age-related decreases in local

gyrification indices within the left ( $r = -.130$ ;  $p = .0004$ ; Fig. 3c) and right PCC/precuneus ( $r = -.132$ ;  $p = .0003$ ; Fig. 3f). In contrast, left ( $r = -.053$ ;  $p = .1512$ ; Fig. 3b) and right AG ( $r = .059$ ;  $p = .1052$ ; Fig. 3e) did not show significant decreases in local gyrification indices with increasing age. Figure 3 shows the relation between residual local gyrification indices (with gender regressed out of the raw local gyrification indices) and age. Thus, the posterior parts of the DMN showed a more pronounced age-related decrease in local gyrification indices than the anterior parts of DMN. Both right hemispheric medial DMN-ROIs showed age-related local gyrification index decline, while only the local gyrification index of the left PCC/precuneus was affected by age.

To test whether the decrease in local gyrification indices in the posterior parts of the DMN were more pronounced than in the anterior parts of DMN and whether right hemispheric parts of the DMN showed more pronounced decreases in local gyrification indices than left hemispheric parts, differences of correlation strength were assessed (using average local gyrification indices across the respective parts of the DMN). We found that the posterior parts of the DMN showed a more pronounced decrease in local gyrification index as compared to the anterior parts of DMN ( $Z = 1.86$ ,  $p = .032$ , one-tailed). Furthermore, the right hemispheric parts of the DMN showed a more pronounced decrease in local gyrification index decrease compared to the left hemispheric parts of the DMN ( $Z = 1.81$ ;  $p = .035$ , one-tailed).

To illustrate the size of these age effects within the raw local gyrification index data, we calculated the mean local gyrification index for every ROI for the 25 % youngest ( $n = 186$ ; male: 95; mean age: 58.9 years  $\pm$  1.37) as well as 25 % oldest subjects ( $n = 190$ ; male: 120; mean age: 76.2 years  $\pm$  2.93). The age effects within the raw local gyrification index data confirm the results shown in the correlation analysis with a more pronounced local gyrification index decrease within the posterior parts of the DMN compared to the anterior parts of DMN and a more pronounced local gyrification index decrease within the right hemispheric parts of the DMN. Overview of raw scores and group comparisons (matched for group size, gender and age decades: 55–64, 65–74, 75–85 years) are presented in Fig. 3g–l.

In addition, we checked for influences of possible cognitive impairment on the effects of age on local gyrification index by adding the total score on a dementia screening test [DemTect, Kalbe et al. (2004)] as a covariate. From all correlations between local gyrification indices and age, and after correcting for multiple comparisons using FDR-correction (Benjamini and Hochberg 1995), the relations between age and local gyrification index still remained significant for the mPFC ( $r = -.125$ ,  $p = .001$ ); left PCC/

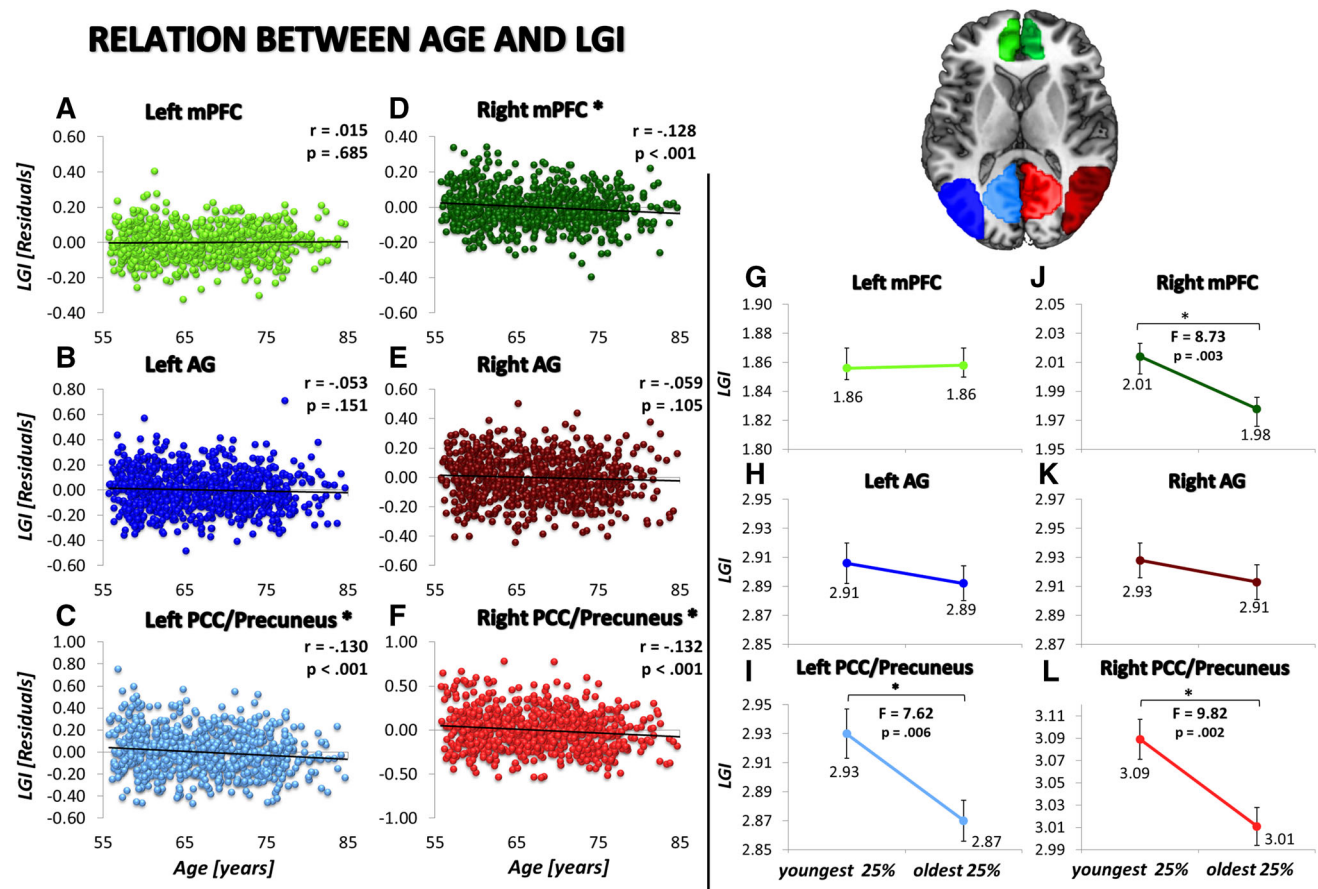


**Fig. 3** Left scatterplots of relation between local gyrification index (LGI; residuals, corrected for gender) and age, with regression lines and correlation coefficients. Right group comparison between

youngest and oldest 25 % of the participants, with raw LGI values and statistical outcomes. Parts of the DMN that were affected by age, using overall and specific analyses are marked with an asterisk

precuneus ( $r = -.125$ ,  $p = .001$ ) and right PCC/precuneus ( $r = -.123$ ,  $p = .001$ ). Thus, even after correcting for global cognitive functioning, age effects on local gyrification index showed a more pronounced local gyrification index decrease within the posterior parts of the DMN and a more pronounced local gyrification index decrease within the right hemispheric parts of the DMN. The comparison between affected parts of the DMN by the overall analysis (without any covariates) and the specific analysis in which we corrected for the DemTect score is displayed in Fig. 5a.

### Effects of cognitive performance

Partial correlations were calculated to assess the relation between cognitive performance and local gyrification indices within the ROIs of the DMN, while correcting for the effects of age and gender. Results were corrected for the number of correlations using FDR correction (6 ROIs  $\times$  14 neuropsychological tests).

Significant correlations were found between the local gyrification indices in the right mPFC, left and right PCC/

precuneus as well as right AG and selective attention, visual and visual-spatial working memory and semantic verbal fluency. Figure 4 displays all significant correlations between cognitive performance and local gyrification indices. Selective attention test scores were negatively correlated with local gyrification index in the left PCC/precuneus ( $r = -.134$ ;  $p = .0003$ ). Visual working memory performance was positively correlated with both the left PCC/precuneus ( $r = .114$ ;  $p = .0018$ ) and the right AG ( $r = .113$ ;  $p = .0019$ ). Visual-spatial working memory performance was positively correlated with local gyrification index in the right PCC/precuneus ( $r = .108$ ;  $p = .0032$ ). Further, semantic verbal fluency was positively correlated with local gyrification indices of the right AG ( $r = .133$ ;  $p = .0003$ ) and right mPFC ( $r = .109$ ;  $p = .0028$ ). All other correlations did not reveal significant results.

In summary, the current results showed significant relations between cognitive performance and all right hemispheric DMN-ROIs. Only the local gyrification index of left PCC/precuneus showed significant correlations to cognitive performance. To illustrate the size of the effects



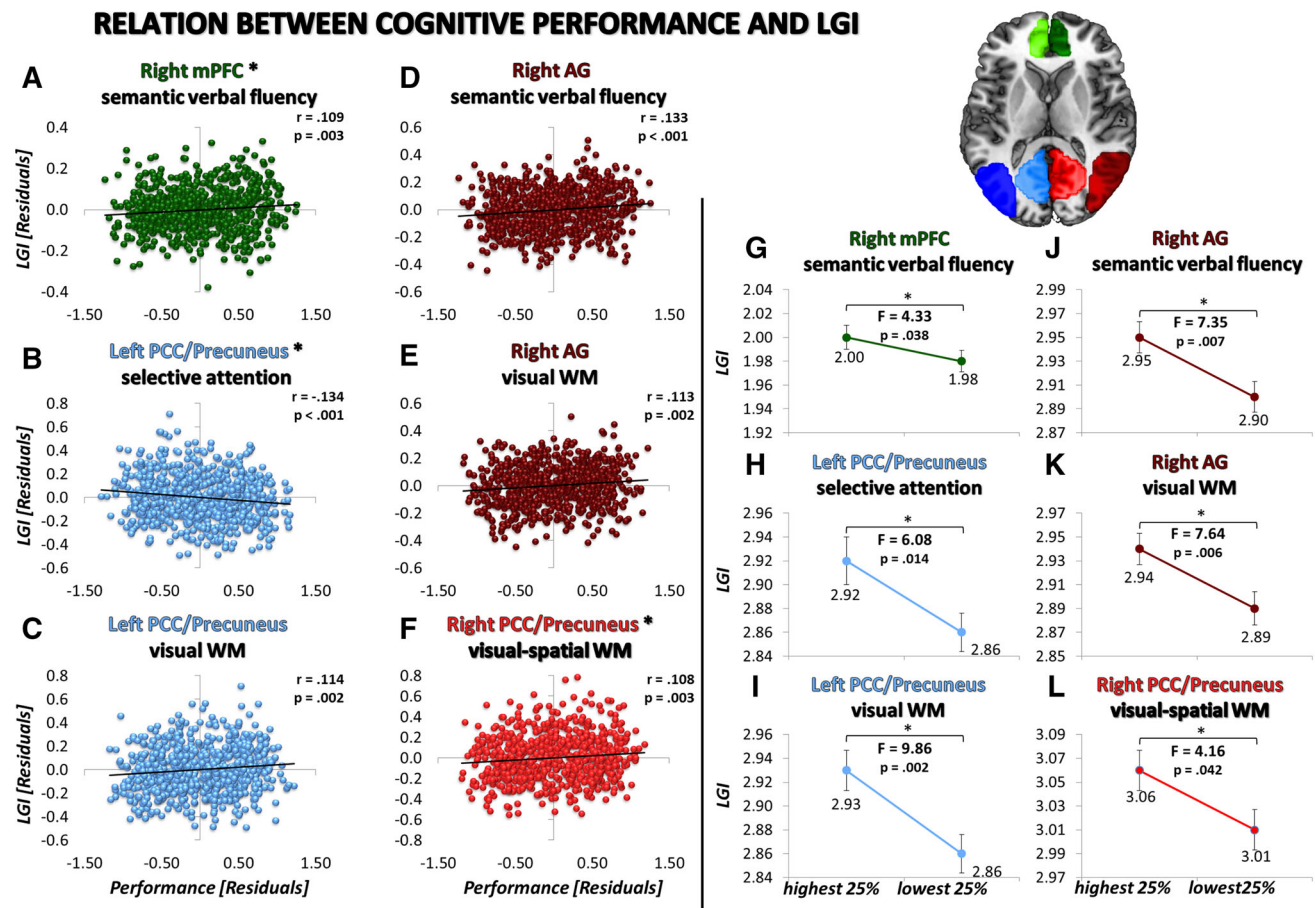


**Fig. 4** *Left* scatterplots of the significant relations between local gyrification index (LGI) values (residuals, corrected for age and gender) and cognitive performance (residuals, corrected for age and gender), with regression lines and correlation coefficients. A higher cognitive performance relates to higher LGI values. *Note* selective attention was measured as time in seconds. Therefore, less time

needed (higher performance) was associated with higher LGI values. Parts of the DMN that were affected by cognitive performance using overall and specific analyses are marked with an *asterisk*. *Right* group comparison between highest and lowest 25 % of the performers, with raw LGI values and statistical outcomes

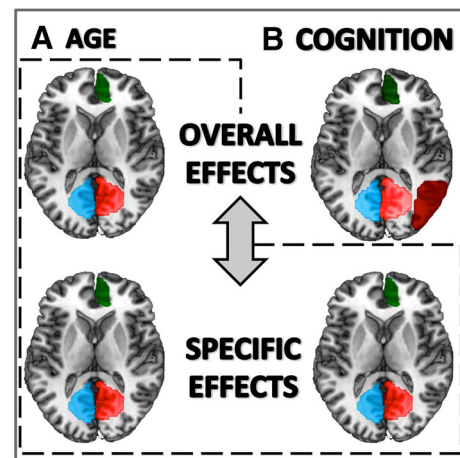
of cognitive performance on local gyrification index, we calculated the mean local gyrification indices for every ROI for the 25 % best performing subjects as well as for the 25 % lowest performing subjects for every significant correlation described above (matched for group size, gender and age decades: 55–64, 65–74, 75–85 years). As a result, the effects of cognitive performance on the raw local gyrification index values confirmed the results derived from the correlation analysis since the local gyrification index decrease was present within all right hemispheric parts of the DMN and the left PCC/precuneus. Overview of raw scores of cognitive performance and group descriptives are presented in Table 2.

To further check whether the main results were biased by those subjects, for whom missing values in the neuropsychological assessment had to be imputed from their

age- and gender-specific peer groups ( $n = 67$ , subjects with more than three missing values were excluded), analyses were repeated without subjects having missing values, including the DemTect score as covariate. Of the six correlations between local gyrification indices and cognitive performance, three were still significant after exclusion of the subjects with missing values (corrected for multiple comparisons using FDR correction), i.e. between selective attention and local gyrification index in the left PCC/precuneus ( $r = -.138$ ,  $p = .0003$ ), visual-spatial working memory and local gyrification index in the right PCC/precuneus ( $r = .125$ ,  $p = .0011$ ), and semantic verbal fluency and local gyrification index in the right mPFC ( $r = .138$ ,  $p = .0003$ ). The comparison between affected parts of the DMN by the overall analysis (including all subjects) and the specific analysis in which we excluded

**Table 2** Mean test scores (raw scores) and group descriptives for the 25 % highest performers and 25 % lowest performers and group comparisons

ROI	Function	Highest 25 % performers		Lowest 25 % performers	
		Test score	Group [n, gender, mean age ( $\pm$ SD)]	Test score	Group [n, gender, mean age ( $\pm$ SD)]
Left PCC/ precuneus	Selective attention (time in s)	24.74 ( $\pm$ 2.30)	n = 123; 60 males, 63 females; 66.82 years ( $\pm$ 6.0)	47.16 ( $\pm$ 9.21)	n = 123; 60 males, 63 females; 67.43 years ( $\pm$ 5.9)
	Visual WM (# correct)	9.55 ( $\pm$ 8.29)	n = 170; 93 males, 77 females; 67.36 years ( $\pm$ 6.36)	5.46 ( $\pm$ 6.30)	n = 170; 93 males, 77 females; 68.32 years ( $\pm$ 6.26)
Right AG	Semantic verbal fluency (# correct)	32.16 ( $\pm$ 4.18)	n = 140; 72 males, 68 females; 67.14 years ( $\pm$ 6.25)	15.70 ( $\pm$ 2.89)	n = 140; 72 males, 68 females; 67.79 years ( $\pm$ 6.49)
	Visual WM (# correct)	9.55 ( $\pm$ 8.29)	n = 170; 93 males, 77 females; 67.36 years ( $\pm$ 6.36)	5.46 ( $\pm$ 6.30)	n = 170; 93 males, 77 females; 68.32 years ( $\pm$ 6.26)
Right PCC/ precuneus	Visual-spatial WM (# correct)	14.36 ( $\pm$ 1.32)	n = 138; 73 males, 65 females; 67.20 years ( $\pm$ 6.51)	7.74 ( $\pm$ 1.42)	n = 138; 73 males, 65 females; 67.94 years ( $\pm$ 6.50)
	Semantic verbal fluency (# correct)	32.16 ( $\pm$ 4.18)	n = 140; 72 males, 68 females; 67.14 years ( $\pm$ 6.25)	15.70 ( $\pm$ 2.89)	n = 140; 72 males, 68 females; 67.79 years ( $\pm$ 6.49)

**Fig. 5** Parts of the DMN that were affected by age and cognitive performance, using overall and specific analyses. *Left* overall analysis of age (including all subjects, covariate: gender) and specific analysis of age (including all subjects, covariates: gender and DemTect). *Right* overall analysis of cognitive performance (including all subjects, covariate: age and gender) and specific analysis (excluding subjects with missing values in the neuropsychological assessment, covariates: age, gender and DemTect)

subjects with missing values and corrected for the DemTect score is displayed in Fig. 5b.

## Discussion

The current study assessed the relation between local gyrification indices and age as well as cognitive performance within the DMN-ROIs (left and right mPFC, PCC/precuneus and AG) in a population-based cohort of older adults. Remarkably, age and cognitive performance showed similar relations to local gyrification indices across the different parts of the DMN: (1) local gyrification indices within posterior parts of DMN showed a stronger relation to age and cognitive performance compared to anterior parts of DMN; and (2) local gyrification indices of right hemispheric DMN-ROIs was stronger correlated with age and cognitive performance than that of the left hemispheric DMN-ROIs.

## Effects of age

In the current study, age-related decreases in local cortical folding were found for right mPFC and bilateral PCC/precuneus. According to previous studies, increasing age leads to increasing brain atrophy, with a similar progression in the left and right hemisphere (Hogstrom et al. 2013; Kochunov et al. 2005, 2008; Liu et al. 2010; Magnotta et al. 1999; Rettmann et al. 2006; Zilles et al. 1988). This is in line with the gyrification decreases found in the current study, but focused on age-related gyrification decline

across different multimodal brain areas encompassed in the DMN. On the one hand, posterior parts of DMN showed a larger age-related local gyrification index decrease than the anterior parts of the DMN. On the other hand, local gyrification index decrease of right hemispheric parts of the DMN was more pronounced than that of the left hemispheric DMN. This hints at local, rather than global age-related decreases of cortical folding within the DMN.

Previous studies discovered changes of the functional organization from early to late adulthood within the DMN (Damoiseaux et al. 2008; Gould et al. 2006; Mowinckel et al. 2012; Sambataro et al. 2010). Interestingly, most of these studies showed increases in resting-state functional connectivity within the anterior part of the DMN. Additionally, age-related decreases of PCC/precuneus activity have been shown (Schlee et al. 2012). As proposed by Davis et al. (2008), the increase in anterior DMN deactivation together with less deactivations of the PCC/precuneus is part of the PASA theory. So, in the brain of older adults the medial PCC/precuneus shows lower (de-) activations as compared to younger subjects. In line with this, PCC/precuneus was found to be vulnerable to age-related gray matter loss (especially within Brodmann area 31) (Mann et al. 2011). With respect to the anterior parts of the DMN, Davis et al. (2008) reported increases in anterior DMN deactivation during task performance in older adults. Thus, while the posterior parts of the DMN seem to show structural decline in older adults, increase in anterior parts of the DMN activation was interpreted as a compensatory mechanism to counteract the structural decline of the posterior parts of the DMN. Following, increases in anterior DMN (de-) activation might be a compensatory attempt to maintain cognitive performance as stable as possible (Ansado et al. 2012; Davis et al. 2008). The current results presented a similar picture, with more pronounced atrophy in PCC/precuneus as compared to mPFC (as measured via decreases in local gyrification index). Thus, the results of the present study provide evidence for a structural correlate of the functionally motivated PASA theory of effects of aging on the brain.

As a second prominent finding, the current study revealed a more pronounced local gyrification index decrease of the right hemispheric parts of the DMN (right: mPFC and PCC/precuneus; left: only PCC/precuneus). Previous research indicated that the right hemisphere might be more prone to age-related decline compared to the left hemisphere, the so-called right-hemi-aging hypothesis (Grady, et al. 1994). Hemispheric asymmetries have been previously reported with regard to structural and functional changes during brain aging. For example, Kovalev et al. (2003) reported accelerated brain aging for right ACC, using MRI texture analysis. Further, Lu et al. (2010) showed that age-related decreases in resting state activity

from 20 to 89 years of age were most notably present within right PFC. Interestingly, when assessing the PASA theory, Davis et al. (2008) found more pronounced deactivation in left mPFC (especially left ACC), which provided evidence for better preserved functioning of left as compared to right hemispheric areas. In line with this, our results of the present study revealed age-related decreases in local gyrification index for right, but not left mPFC. Thus, left mPFC might be an important driving factor for any compensatory process, as it is less affected by age-related atrophy, supporting the right hemi-aging theory. Nevertheless, it has to be noted, that the right-hemi-aging hypothesis is mainly based on behavioral observations showing that right-hemispheric cognitive processes, such as spatial processing are markedly affected during aging. Thus, further research is necessary to explore the relationship between cognitive decline according to the right hemi-aging theory, functional reorganization in the aging brain, and age-related structural atrophy, as reflected by the results of the present study.

Taken together, the current results provided evidence for more pronounced decrease in local gyrification index in the posterior as compared to the anterior parts of the DMN—supporting the functionally based PASA theory—as well as in right as compared to left hemispheric parts of the DMN—supporting the right-hemi-aging model.

### Effects of cognitive performance on local gyrification indices

In the current study, significant correlations between local gyrification indices and cognitive performance were found in largely the same parts of the DMN as already found for the correlation of local gyrification index with age. Performance in the domain of attention was positively correlated with local gyrification index of left PCC/precuneus. Better working memory performance correlated with a higher local gyrification index of PCC/precuneus and right AG, and better performance in language performance positively correlated with local gyrification index in right mPFC and right AG.

Like for the age-related decreases in local gyrification indices, cognitive performance was more pronouncedly related to local gyrification indices in posterior as compared to anterior parts of the DMN. Local gyrification index decreases of posterior parts of the DMN (bilateral PCC/precuneus and right AG) were related to deficits in selective attention, as well as visual and visual-spatial working memory performance. Functionally, the DMN as such and the PCC/precuneus in particular, seem to be strongly involved in attentional processes (Buckner et al. 2008, 2009). Moreover, the involvement of the AG in visual processing has also been explored. For example, the

transmitter receptor distribution of AG is similar to that of the extrastriate visual brain areas, indicating the AG to be involved in visual processing (Caspers et al. 2013). During aging, deficits in early visual processing stages seem to impair visual working memory performance (Gazzaley et al. 2008; Gazzaley and Nobre 2012). Further, it was shown that a lack of desynchronization of brain oscillatory activity within PCC/precuneus and right AG disrupts the efficient processing within the fronto-parietal working memory network, leading to a decline in visual working memory performance (Pinal et al. 2015).

Thus, the current study revealed cognitive performance-related local gyrification index decreases in the posterior parts of the DMN (bilateral PCC/precuneus and right AG). The bilateral PCC/precuneus and right AG were functionally shown to be involved in the processing of visual working memory and visual attention. Additionally, subjects with a lower local gyrification in these brain areas in our sample also showed a lower performance in visual working memory and attention. Relating the current study to the aforementioned functional imaging study, it might be assumed that low performers also show functional impairments in brain networks involved in visual working memory and visual attention. This observation would be also in line with the PASA hypothesis, since PASA suggests a more pronounced atrophy within posterior brain regions to be associated with cognitive performance decline. However, further research is necessary to test the exact function-structure relationship with respect to PASA.

Further, the correlations between local gyrification decreases and cognitive performance complement those found for age: gyrification in posterior as compared to anterior parts of the DMN were not only more prone to age-related alterations, but were also found to relate to specific cognitive performance decline. Thus, the present results hint at a structural correlate of the functionally established PASA theory in a large cohort of older adults in two aspects: (1) with regard to an integrated view on structure–function reorganization in the older adults' brain; and (2) in relation to its behavioral performance outcome.

Similar to the age effects, the relation between cognitive performance and local gyrification revealed a second prominent finding: local gyrification indices of all right hemispheric DMN-ROIs were correlated to cognitive performance decline, as compared to only a relation between local gyrification index of the PCC/precuneus in the left hemisphere. This, again, is in line with the right hemi-aging theory. The local gyrification indices of the right PCC/precuneus and AG were associated with visual (-spatial) working memory. The right hemi-aging theory, which is mainly built on behavioral observations, states a

prominent and earlier decline of visual–spatial cognitive processes, compared to language processes (Dolcos et al. 2002). The authors explained these effects by an earlier and more pronounced decline of right hemispheric functions, which should be associated with earlier and more prominent changes of the structural or functional architecture of the right as compared to the left hemisphere. The current results fit to this hypothesis, because the right PCC/precuneus and AG were positively correlated to visual–spatial working memory performance. Although the right hemi-aging theory is widely debated, especially in functional imaging [e.g. Dolcos et al. (2002)] the current results are further supported by Li et al. (2009). In this study, structural and functional connectivity was investigated in older adults. A right hemispheric fronto-parietal structural connectivity reduction was found in older compared to younger adults. Our results might add to this finding in that we found predominant grey matter atrophy in right as compared to left fronto-parietal regions. In addition, more pronounced atrophy of white matter in the right as compared to the left hemisphere, especially in the right frontal lobe, was associated with verbal and nonverbal cognitive performance decline (Brickman et al. 2006). The results of the present study further amend these previous findings by showing that also cortical structure of left and right hemisphere might be differentially affected during aging. As this was shown here for the default mode network, future studies might yield further insight if right hemi-aging is a global or rather local process during aging, at this differentially affecting cognitive performance in older adults. Additionally, intra-subject trajectories of structural changes of right versus left hemispheric regions could be assessed in a longitudinal design to further elucidate if aging processes indeed happen earlier in the right than in the left hemisphere.

Interestingly, local gyrification indices of the right mPFC and AG were positively correlated to performance in semantic verbal fluency. Functionally, the AG has strongly been associated with semantic verbal fluency (Binder et al. 2009; Shalom and Poeppel 2008; for a recent review see Seghier 2013). Nevertheless, age-related decline of the anterior part of the DMN (i.e. ACC) has also been shown to be correlated to verbal fluency scores (Pardo et al. 2007). However, contrary to the current results, previous studies showed a more prominent involvement of left mPFC and AG in semantic verbal fluency tasks (Binder et al. 2009; Wagner et al. 2014). Even though the relation between local gyrification indices of right mPFC and AG and cognitive performance seems to fit with the right hemi-aging hypothesis, it remains questionable why only the right hemispheric DMN-ROIs related to cognitive performance in a task which is known to involve mainly left hemispheric brain areas. Most of the aforementioned

studies focused on subjects younger than those included in the current study. It is known in older adults, though, that a more bilateral recruitment of brain regions is necessary to maintain performance in cognitively demanding tasks as high as in younger subjects (HAROLD-Model; Hemispheric-asymmetry-reduction-in-older-adults) (Cabeza 2002). Relating this to the current results, it might be assumed that right AG and mPFC gain importance in semantic verbal fluency performance in older adults. Consequently, a more pronounced atrophy of these brain regions (according to the right-hemi-aging theory) would lead to a loss of relevant additional functional recruitment (according to HAROLD), and would impair performance in the older adults. In summary, similar to the age-related local gyrification index decreases within the DMN, local gyrification index of posterior as compared to anterior parts of the DMN showed stronger correlations to cognitive performance decline, supporting PASA. Furthermore, local gyrification index of all right hemispheric parts of the DMN correlated to cognitive performance decline, strengthening the right-hemi-aging model.

Finally, it has to be mentioned that the current study was designed as a population-based study. Thus, we did not exclude subjects based on any criteria except from claustrophobia and contraindications to the MR. Since some of the participants had missing values on the neuropsychological assessment ( $n = 67$ ) we re-ran the correlation analyses of cognitive performance and local gyrification indices, while excluding these participants from the analysis. In addition, it might be possible that global cognitive functioning had an influence. Therefore, we additionally included the DemTect as a covariate in the analysis of age as well as cognitive performance (see above on the discussion of “Effects of age”). This additional analysis revealed an interesting finding: the same DMN-ROIs that were affected by the factor “age” were affected by cognitive performance (cf. Fig. 5). Thus, the more conservative approach including only those subjects who had all neuropsychological test data available, re-focused the findings to a core of brain regions in which local gyrification was robustly associated with cognitive performance. This stepwise inclusion of potential influencing factors, which might be relevant when studying relation between cortical folding and age or cognitive performance, thus further strengthens the idea that there might be a structural correlate for the PASA as well as for the right hemi-aging theory. It remains for future studies to further establish if and in which groups of subjects cognitive performance might be additionally associated with structural brain changes, as could be assumed based on our results when including all subjects in the analyses, for whom stratified neuropsychological test scores were imputed.

## Methodological issues

The current study has several advantages and limitations which should be addressed. First, the effects of age as well as cognitive performance only explained small parts of the total variance in this sample. Although results are statistically significant, even after correction for multiple comparisons, the factors “age” and “cognitive performance” could not explain the same amount of variance in local gyrification as it was shown for the whole lifespan from early to late adulthood (Hogstrom et al. 2013). However, it has to be noted that in comparison to other studies, investigating young versus older adults, the current sample investigated age effects in a sample consisting of older adults only. Previous studies already showed that the effects of age on brain structure do not necessarily follow a linear relationship from early to late life, with smaller rates of brain atrophy in older adults [e.g. Sowell et al. (2003)]. The reliable detection of subtle, but relevant, effects in local gyrification requires large sample sizes (Button et al. 2013). Given the large number of older adults investigated (i.e. 55 years and above), the present study did indeed have sufficient power to demonstrate small effects of age and cognitive performance on local gyrification in a population-based sample of older adults. These effects might nevertheless provide relevant impact on brain structure in older adults as part of the inter-individual variability, together with other factors that might influence brain atrophy in older subjects, such as genetic variations, environment or lifestyle. With each of them having only a small effect, they all could add up to finally give an overall picture of the inter-individual variability of brain phenotypes in late decades of life. Further studies are warranted to assess the particular relevance of these significant but small effects for structural or functional reorganization in the aging brain.

A second important point that has to be discussed is the population-based design of the present study. The examined cohort represents a high inter-individual variability across normal older adults. In contrast to other study designs, e.g. case–control designs, the advantage of population-based cohort studies is to assess influencing factors for brain aging in the normal population, with a high generalizability. While exploring such influences in the population, a basis of the normal aging process of the brain can be established, which is necessary to better characterize the normal range of aging within the assumed continuous spectrum from health to disease (Tucker and Stern 2011). However, taking such a global approach across the general population could bear the chance of showing only global effects, while more specific findings might be disregarded, e.g. an effect such as global cognitive impairment. Therefore, using a stepwise inclusion/exclusion

approach of factors that might bias the results is of particular interest in a population-based design such as the present study. We used this stepwise approach by including additional covariates, such as the DemTect, and by excluding participants who had missing values in the neuropsychological data since it helped to further differentiate between overall and more specific effects (cf. Fig. 5).

Moreover, the cross-sectional design of the present study did not allow for investigating the intra-individual course of cognitive decline and changes in local gyrification index during aging. Future research on longitudinal data could thus further elucidate the individual trajectories of local gyrification index in older adults in relation to age and cognitive performance. Furthermore, the current study draws inferences on the local gyrification index of DMN regions. It remains for future studies to investigate regional susceptibility of local gyrification index to age and cognitive performance in other cognitive brain networks, e.g. frontoparietal resting state networks.

## Conclusions

The current study assessed gyrification of the DMN in relation to age and cognitive performance in an older adults' population-based sample. Age-related structural decline was more pronounced within posterior as compared to anterior parts of the DMN, providing a structural correlate for the functionally established PASA theory. Further, the prominent structural decline in right hemispheric ROIs of the DMN is in accordance with the right hemi-aging model. Beyond age, cognitive performance-related changes in local gyrification index were present in largely the same parts of the DMN that were already more vulnerable to age-related local gyrification decreases. First, local gyrification index decreases in posterior parts of the DMN were related to performance decline in visual (-spatial) working memory and selective attention, supporting the PASA theory. Second, local gyrification index decreases of right hemispheric DMN-ROIs were correlated to performance decline in semantic verbal fluency, supporting the right hemi-aging-theory. Thus, age and cognitive performance-related local gyrification index decreases provide structural correlates for PASA and the right-hemi-aging theory. The present study therefore suggests common underlying processes of reorganization in the older adults brain, encompassing brain structure and function as well as related performance outcome.

**Acknowledgments** This project was partially funded by the German National Cohort and the 1000BRAINS-Study of the Institute of Neuroscience and Medicine, Research Centre Jülich, Germany. We

thank the Heinz Nixdorf Foundation (Germany) for the generous support of the Heinz Nixdorf Recall Study. The study is also supported by the German Ministry of Education and Science. Assessment of psychosocial factors and neighborhood level information is funded by the German Research Council (DFG; Project SI 236/8-1 and SI236/9-1 and ER 155/6-1, 6-2). The research leading to these results has received funding from the European Union Seventh Framework Programme (FP7/2007–2013) under Grant Agreement No. 604102 (Human Brain Project). We thank the investigative group and the study staff of the Heinz Nixdorf Recall Study.

## References

- Amft M, Bzdok D, Laird AR, Fox PT, Schilbach L, Eickhoff SB (2015) Definition and characterization of an extended social-affective default network. *Brain Struct Funct* 220:1031–1049
- Amunts K, Malikovic A, Mohlberg H, Schormann T, Zilles K (2000) Brodmann's areas 17 and 18 brought into stereotaxic space-where and how variable? *NeuroImage* 11(1):66–84
- Andrews-Hanna JR, Snyder AZ, Vincent JL, Lustig C, Head D, Raichle ME, Buckner RL (2007) Disruption of large-scale brain systems in advanced aging. *Neuron* 56:924–935
- Ansado J, Monchi O, Ennabil N, Faure S, Joannette Y (2012) Load-dependent posterior–anterior shift in aging in complex visual selective attention situations. *Brain Res* 1454:14–22
- Aschenbrenner A, Tucha O, Lange K (2000) RWT Regensburger Wortflüssigkeits-Test. Göttingen
- Bai F, Zhang Z, Yu H, Shi Y, Yuan Y, Zhu W, Qian Y (2008) Default-mode network activity distinguishes amnesic type mild cognitive impairment from healthy aging: a combined structural and resting-state functional MRI study. *Neurosci Lett* 438(1):111–115
- Batouli AH, Boroomand A, Fakhri M, Sikaroodi H, Oghabian MA, Firouznia K (2009) The effect of aging on resting-state brain function: an fMRI study. *Iran J Radiol* 6(3):153–158
- Beckmann CF, Smith SM (2004) Probabilistic independent component analysis for functional magnetic resonance imaging. *IEEE Trans Med Imaging* 23(2):137–152
- Beckmann CF, DeLuca M, Devlin JT, Smith SM (2005) Investigations into resting-state connectivity using independent component analysis. *Philos Trans R Soc Lond* 360(1457):1001–1013
- Benjamini Y, Hochberg Y (1995) Controlling the false discovery rate: a practical and powerful approach to multiple testing. *J R Stat Soc* 57(1):289–300
- Benton AL, Sivan AB, Spreen O, Steck P (2009) Der Benton-Test Huber, Hogrefe
- Binder JR, Desai RH, Graves WW, Conant LL (2009) Where is the semantic system? A critical review and meta-analysis of 120 functional neuroimaging studies. *Cereb Cortex* 19(12):2767–2796
- Bludau S, Eickhoff SB, Mohlberg H, Caspers S, Laird AR, Fox PT et al (2014) Cytoarchitecture, probability maps and functions of the human frontal pole. *NeuroImage* 93:260–275
- Brickman AM, Zimmerman ME, Paul RH, Grieve SM, Tate DF, Cohen RA, Gordon E (2006) Regional white matter and neuropsychological functioning across the adult lifespan. *Biol Psychiatry* 60(5):444–453
- Buckner RL, Andrews-Hanna JR, Schacter DL (2008) The brain's default network: anatomy, function, and relevance to disease. *Ann N Y Acad Sci* 1124:1–38
- Buckner RL, Sepulcre J, Talukdar T, Krienen FM, Liu H, Hedden T, Johnson KA (2009) Cortical hubs revealed by intrinsic functional connectivity: mapping, assessment of stability, and relation to Alzheimer's disease. *J Neurosci* 29(6):1860–1873

- Button KS, Ioannidis JP, Mokrysz C, Nosek BA, Flint J, Robinson ES, Munafò MR (2013) Power failure: why small sample size undermines the reliability of neuroscience. *Nat Rev Neurosci* 14(5):365–376
- Cabeza R (2002) Hemispheric asymmetry reduction in older adults: the HAROLD model. *Psychol Aging* 17(1):85–100
- Caspers S, Geyer S, Schleicher A, Mohlberg H, Amunts K, Zilles K (2006) The human inferior parietal cortex: cytoarchitectonic parcellation and interindividual variability. *NeuroImage* 33(2):430–448
- Caspers S, Eickhoff SB, Geyer S, Scheperjans F, Mohlberg H, Zilles K et al (2008) The human inferior parietal lobule in stereotaxic space. *Brain Struct Funct* 212(6):481–495
- Caspers S, Schleicher A, Bacha-Trams M, Palomero-Gallagher N, Amunts K, Zilles K (2013) Organization of the human inferior parietal lobule based on receptor architectonics. *Cereb Cortex* 23(3):615–628
- Caspers S, Moebus S, Lux S, Pundt N, Schutz H, Muhleisen TW, Amunts K (2014) Studying variability in human brain aging in a population-based German cohort—rationale and design of 1000BRAINS. *Front Aging Neurosci* 6:149
- Dale AM, Fischl B, Sereno MI (1999) Cortical surface-based analysis. I. Segmentation and surface reconstruction. *NeuroImage* 9(2):179–194
- Damoiseaux JS, Beckmann CF, Arigita EJ, Barkhof F, Scheltens P, Stam CJ, Rombouts SA (2008) Reduced resting-state brain activity in the “default network” in normal aging. *Cereb Cortex* 18(8):1856–1864
- Davis SW, Dennis NA, Daselaar SM, Fleck MS, Cabeza R (2008) Que PASA? The posterior–anterior shift in aging. *Cereb Cortex* 18(5):1201–1209
- Della Sala S, Gray C, Baddeley AD, Wilson L (1997) The visual patterns test: a test of short-term visual recall. Thames Valley Test Company
- Docherty AR, Hagler DJ Jr, Panizzon MS, Neale MC, Eyer LT, Fennema-Notestine C, Franz CE, Jak A, Lyons MJ, Rinker DA, Thompson WK, Tsuang MT, Dale AM, Kremen WS (2015) Does degree of gyrification underlie the phenotypic and genetic associations between cortical surface area and cognitive ability? *Neuroimage* 106:154–160
- Dolcos F, Rice HJ, Cabeza R (2002) Hemispheric asymmetry and aging: right hemisphere decline or asymmetry reduction. *Neurosci Biobehav Rev* 26(7):819–825
- Eickhoff SB, Stephan KE, Mohlberg H, Grefkes C, Fink GR, Amunts K, Zilles K (2005) A new SPM toolbox for combining probabilistic cytoarchitectonic maps and functional imaging data. *NeuroImage* 25(4):1325–1335
- Fischl B, Sereno MI, Dale AM (1999) Cortical surface-based analysis. II: inflation, flattening, and a surface-based coordinate system. *NeuroImage* 9(2):195–207
- Gatterer G, Fischer P, Simanyi M, Danielczyk W (1989) The A-K-T (“Alters-Konzentrations-Test”) a new psychometric test for geriatric patients. *Funct Neurol* 4(3):273–276
- Gazzaley A, Nobre AC (2012) Top-down modulation: bridging selective attention and working memory. *Trends Cognit Sci* 16(2):129–135
- Gazzaley A, Clapp W, Kelley J, McEvoy K, Knight RT, D’Esposito M (2008) Age-related top-down suppression deficit in the early stages of cortical visual memory processing. *Proc Natl Acad Sci USA* 105(35):13122–13126
- Gould RL, Brown RG, Owen AM, Bullmore ET, Howard RJ (2006) Task-induced deactivations during successful paired associates learning: an effect of age but not Alzheimer’s disease. *NeuroImage* 31(2):818–831
- Grady CL, Maisog JM, Horwitz B, Ungerleider LG, Mentis MJ, Salerno JA, Haxby JV (1994) Age-related changes in cortical blood flow activation during visual processing of faces and location. *J Neurosci* 14(3 Pt 2):1450–1462
- Grady CL, Springer MV, Hongwanishkul D, McIntosh AR, Winocur G (2006) Age-related changes in brain activity across the adult lifespan. *J Cogn Neurosci* 18(2):227–241. doi:10.1162/089892906775783705
- Griffanti L, Salimi-Khorshidi G, Beckmann CF, Auerbach EJ, Douaud G, Sexton CE, Smith SM (2014) ICA-based artefact removal and accelerated fMRI acquisition for improved resting state network imaging. *NeuroImage* 95:232–247
- Hedden T, Gabrieli JD (2004) Insights into the ageing mind: a view from cognitive neuroscience. *Nat Rev Neurosci* 5(2):87–96
- Himberg J, Hyvarinen A. 2003. ICASSO: software for investigating the reliability of ICA estimates by clustering and visualization. In: 2003 IEEE Xiii workshop on neural networks for signal processing—Nnsp’03, pp 259–268
- Hoerger M (2013) Z<sub>H</sub>: an updated version of Steiger’s Z and web-based calculator for testing the statistical significance of the difference between dependent correlations. [http://www.psychmike.com/dependent\\_correlations.php](http://www.psychmike.com/dependent_correlations.php)
- Hogstrom LJ, Westlye LT, Walhovd KB, Fjell AM (2013) The structure of the cerebral cortex across adult life: age-related patterns of surface area, thickness, and gyrification. *Cereb Cortex* 23(11):2521–2530
- Jenkinson M, Smith S (2001) A global optimisation method for robust affine registration of brain images. *Med Image Anal* 5(2):143–156
- Jenkinson M, Bannister P, Brady M, Smith S (2002) Improved optimization for the robust and accurate linear registration and motion correction of brain images. *NeuroImage* 17(2):825–841
- Jenkinson M, Beckmann CF, Behrens TE, Woolrich MW, Smith SM (2012) Fsl. *NeuroImage* 62(2):782–790
- Jones DT, Machulda MM, Vemuri P, McDade EM, Zeng G, Senjem ML, Jack CR Jr (2011) Age-related changes in the default mode network are more advanced in Alzheimer disease. *Neurology* 77(16):1524–1531
- Kalbe E, Kessler J, Calabrese P, Smith R, Passmore AP, Brand M, Bullock R (2004) DemTect: a new, sensitive cognitive screening test to support the diagnosis of mild cognitive impairment and early dementia. *Int J Geriatr Psychiatry* 19:136–143
- Kochunov P, Mangin JF, Coyle T, Lancaster J, Thompson P, Riviere D, Fox PT (2005) Age-related morphology trends of cortical sulci. *Hum Brain Mapp* 26(3):210–220
- Kochunov P, Thompson PM, Coyle TR, Lancaster JL, Kochunov V, Royall D, Fox PT (2008) Relationship among neuroimaging indices of cerebral health during normal aging. *Hum Brain Mapp* 29(1):36–45
- Kovalev VA, Kruggel F, von Cramon DY (2003) Gender and age effects in structural brain asymmetry as measured by MRI texture analysis. *NeuroImage* 19(3):895–905
- Kujovic M, Zilles K, Malikovic A, Schleicher A, Mohlberg H, Rottschy C et al (2013) Cytoarchitectonic mapping of the human dorsal extrastriate cortex. *Brain Struct Funct* 218(1):157–172
- Li Z, Moore AB, Tyner C, Hu X (2009) Asymmetric connectivity reduction and its relationship to “HAROLD” in aging brain. *Brain Res* 1295:149–158
- Liu T, Wen W, Zhu W, Trollor J, Reppermund S, Crawford J, Sachdev P (2010) The effects of age and sex on cortical sulci in the elderly. *NeuroImage* 51(1):19–27
- Lux S, Hartje W, Reich C, Nagel C (2012) VGT: Verbaler Gedächtnistest: Bielefelder Kategoriale Wortlisten. Hogrefe, Göttingen
- Lu H, Xu F, Rodrigue KM, Kennedy KM, Cheng Y, Flicker B, Park DC (2010) Alterations in cerebral metabolic rate and blood supply across the adult lifespan. *Cereb Cortex* 21(6):1426–1434
- Lustig C, Snyder AZ, Bhakta M, O’Brien KC, McAvoy M, Raichle ME, Buckner RL (2003) Functional deactivations: change with

- age and dementia of the Alzheimer type. *Proc Natl Acad Sci USA* 100(24):14504–14509
- Magnotta VA, Andreasen NC, Schultz SK, Harris G, Cizadlo T, Heckel D, Flaum M (1999) Quantitative in vivo measurement of gyrfication in the human brain: changes associated with aging. *Cereb Cortex* 9(2):151–160
- Malikovic A, Amunts K, Schleicher A, Mohlberg H, Eickhoff SB, Wilms M et al (2007) Cytoarchitectonic analysis of the human extrastriate cortex in the region of V5/MT+: a probabilistic, stereotaxic map of area hOc5. *Cereb Cortex* 17(3):562–574
- Mann SL, Hazlett EA, Byne W, Hof PR, Buchsbaum MS, Cohen BH, Siever LJ (2011) Anterior and posterior cingulate cortex volume in healthy adults: effects of aging and gender differences. *Brain Res* 1401:18–29
- Mével K, Chetelat G, Eustache F, Desgranges B (2011) The default mode network in healthy aging and Alzheimer's disease. *Int J Alzheimer's Dis* 2011:535816
- Morris JC, Heyman A, Mohs RC, Hughes JP, Van Belle G, Fillenbaum G, Clark C, The CERAD investigators (1989) The consortium to establish a registry for alzheimer's disease (CERAD). Part I. Clinical and neuropsychological assessment of Alzheimer's disease. *Neurology* 39(9):1159–1165
- Mowinckel AM, Espeseth T, Westlye LT (2012) Network-specific effects of age and in-scanner subject motion: a resting-state fMRI study of 238 healthy adults. *NeuroImage* 63(3):1364–1373
- Oswald WD, Fleischmann UM (1997) Das Nürnberger-Alters-Inventar (NAI) Hogrefe, Göttingen
- Palaniyappan L, Liddle PF (2012) Aberrant cortical gyrfication in schizophrenia: a surface-based morphometry study. *J Psychiatry Neurosci* 37(6):399–406
- Palaniyappan L, Marques TR, Taylor H, Handley R, Mondelli V, Bonaccorso S, Dazzan P (2013) Cortical folding defects as markers of poor treatment response in first-episode psychosis. *JAMA Psychiatry* 70(10):1031–1040
- Palomero-Gallagher N, Eickhoff SB, Hoffstaedter F, Schleicher A, Mohlberg H, Vogt BA et al (2015) Functional organization of human subgenual cortical areas: relationship between architectural segregation and connective heterogeneity. *NeuroImage* 115:177–190
- Pardo JV, Lee JT, Sheikh SA, Surerus-Johnson C, Shah H, Munch KR, Dysken MW (2007) Where the brain grows old: decline in anterior cingulate and medial prefrontal function with normal aging. *NeuroImage* 35(3):1231–1237
- Pinal D, Zurrón M, Diaz F, Sauseng P (2015) Stuck in default mode: inefficient cross-frequency synchronization may lead to age-related short-term memory decline. *Neurobiol Aging* 36(4):1611–1618
- Raichle ME, MacLeod AM, Snyder AZ, Powers WJ, Gusnard DA, Shulman GL (2001) A default mode of brain function. *Proc Natl Acad Sci USA* 98(2):676–682
- Regard M, Strauss E, Knapp P (1982) Children's production on verbal and non-verbal fluency tasks. *Percept Motor Skills* 55(3 Pt 1):839–844
- Rettmann ME, Kraut MA, Prince JL, Resnick SM (2006) Cross-sectional and longitudinal analyses of anatomical sulcal changes associated with aging. *Cereb Cortex* 16(11):1584–1594
- Saenger VM, Barrios FA, Martínez-Gudiño ML, Alcauter S (2012) Hemispheric asymmetries of functional connectivity and grey matter volume in the default mode network. *Neuropsychologia* 50:1308–1315
- Salimi-Khorshidi G, Douaud G, Beckmann CF, Glasser MF, Griffanti L, Smith SM (2014) Automatic denoising of functional MRI data: combining independent component analysis and hierarchical fusion of classifiers. *NeuroImage* 90:449–468
- Sambataro F, Murty VP, Callicott JH, Tan HY, Das S, Weinberger DR, Mattay VS (2010) Age-related alterations in default mode network: impact on working memory performance. *Neurobiol Aging* 31(5):839–852
- Schaer M, Cuadra MB, Tamarit L, Lazeyras F, Eliez S, Thiran JP (2008) A surface-based approach to quantify local cortical gyrfication. *IEEE Trans Med Imaging* 27(2):161–170
- Schaer M, Cuadra MB, Schmansky N, Fischl B, Thiran JP, Eliez S (2012) How to measure cortical folding from MR images: a step-by-step tutorial to compute local gyrfication index. *J Vis Exp* 59:e3417
- Schelling D (1997) Block-tapping-test. Swets Test Service GmbH, Frankfurt
- Scheperjans F, Eickhoff SB, Homke L, Mohlberg H, Hermann K, Amunts K et al (2008a) Probabilistic maps, morphometry, and variability of cytoarchitectonic areas in the human superior parietal cortex. *Cereb Cortex* 18(9):2141–2157
- Scheperjans F, Hermann K, Eickhoff SB, Amunts K, Schleicher A, Zilles K (2008b) Observer-independent cytoarchitectonic mapping of the human superior parietal cortex. *Cereb Cortex* 18(4):846–867
- Schilbach L, Bzdok D, Timmermans B, Fox PT, Laird AR, Vogeley K, Eickhoff SB (2012) Introspective minds: using ALE meta-analyses to study commonalities in the neural correlates of emotional processing, social and unconstrained cognition. *PLoS One* 7:e30920
- Schlee W, Leirer V, Kolassa IT, Weisz N, Elbert T (2012) Age-related changes in neural functional connectivity and its behavioral relevance. *BMC Neurosci* 13:16
- Schmermund A, Möhlenkamp S, Stang A, Gronemeyer D, Seibel R, Hirche H, Invest HNRS (2002) Assessment of clinically silent atherosclerotic disease and established and novel risk factors for predicting myocardial infarction and cardiac death in healthy middle-aged subjects: rationale and design of the Heinz Nixdorf RECALL Study. *Am Heart J* 144(2):212–218
- Schmidt K-H, Metzler P (1992) Wortschatztest: WST: Beltz
- Seghier ML (2013) The angular gyrus: multiple functions and multiple subdivisions. *The Neuroscientist* 19(1):43–61
- Shalom DB, Poeppel D (2008) Functional anatomic models of language: assembling the pieces. *The Neuroscientist* 14(1):119–127
- Smith SM (2002) Fast robust automated brain extraction. *Hum Brain Mapp* 17(3):143–155
- Smith SM, Fox PT, Miller KL, Glahn DC, Fox PM, Mackay CE, Beckmann CF (2009) Correspondence of the brain's functional architecture during activation and rest. *Proc Natl Acad Sci USA* 106(31):13040–13045
- Sowell ER, Peterson BS, Thompson PM, Welcome SE, Henkenius AL, Toga AW (2003) Mapping cortical change across the human life span. *Nat Neurosci* 6(3):309–315
- Steiger JH (1980) Tests for comparing elements of a correlation matrix. *Psychol Bull* 87:245–251
- Stroop JR (1935) Studies of interference in serial verbal reactions. *J Exp Psychol* 18:643–662
- Sturm W, Willmes K, Horn W (1993) Leistungsprüfungssystem für 50–90jährige. Handanweisung, 2nd edn. Hogrefe, Göttingen
- Tucker AM, Stern Y (2011) Cognitive reserve in aging. *Curr Alzheimer Res* 8:354–360
- Van Essen DC (1997) A tension-based theory of morphogenesis and compact wiring in the central nervous system. *Nature* 385(6614):313–318
- Wagner S, Sebastian A, Lieb K, Tuscher O, Tadic A (2014) A coordinate-based ALE functional MRI meta-analysis of brain activation during verbal fluency tasks in healthy control subjects. *BMC Neurosci* 15:19
- Welker W (1990) Why does cerebral cortex fissure and fold? In: Jones E, Peters A (eds) cerebral cortex, vol 8B. Springer, New York, pp 3–136



- White T, Su S, Schmidt M, Kao CY, Sapiro G (2010) The development of gyrification in childhood and adolescence. *Brain Cogn* 72(1):36–45
- Wu JT, Wu HZ, Yan CG, Chen WX, Zhang HY, He Y, Yang HS (2011) Aging-related changes in the default mode network and its anti-correlated networks: a resting-state fMRI study. *Neurosci Lett* 504(1):62–67
- Zhang Y, Zhang J, Xu J, Wu X, Feng H, Wang J, Jiang T (2014) Cortical gyrification reductions and subcortical atrophy in Parkinson's disease. *Mov Disord* 29(1):122–126
- Zilles K, Amunts K (2010) Centenary of Brodmann's map—conception and fate. *Nat Rev Neurosci* 11(2):139–145
- Zilles K, Palomero-Gallagher N (2015) Gyrification in the human brain. In: Toga AW (ed) *Brain mapping: an encyclopedic reference*. In: Zilles K, Amunts K (eds) *Section anatomy and physiology*, Chap 197. Elsevier Academic Press, San Diego, pp 37–44
- Zilles K, Armstrong E, Schleicher A, Kretschmann HJ (1988) The human pattern of gyrification in the cerebral cortex. *Anat Embryol* 179(2):173–179
- Zilles K, Palomero-Gallagher N, Amunts K (2013) Development of cortical folding during evolution and ontogeny. *Trends Neurosci* 36(5):275–284